853

Initial Analysis and Forecasts of the 31 May 2013 El Reno Tornadic Storm: Impact from Rapid-Scan Phased Array Radar (PAR)

Patrick S. Skinner, Louis J. Wicker, Pamela L. Heinselman, and David J. Stensrud
NOAA/National Severe Storms Laboratory

Experiment Overview

The capability of multifunction phased-array radar (MPAR) to collect high temporal resolution, volumetric data of high-impact weather (Heinselman and Torres 2011) makes it an attractive platform for use in convective-scale data assimilation. Assimilation of MPAR data has been shown to improve analyses and forecasts of tornado potential in both observing system simulation (Yussouf and Stensrud 2010) and real-data (Wicker et al. 2014) experiments which, coupled with the potential of MPAR to serve as a next-generation weather surveillance network suggests that it will be important to the development of ensemble-based probabalistic hazard guidance or Warn-on-Forecast (Stensrud et al. 2009, 2013).

Towards this goal, this study will present initial forecasts of the 31 May 2013 El Reno, Oklahoma tornadic supercell initialized by assimilating MPAR data into the NCOMMAS (Coniglio et al. 2006) model using a Local Ensemble Transform Kalman Filter (LETKF) (Hunt et al. 2007)

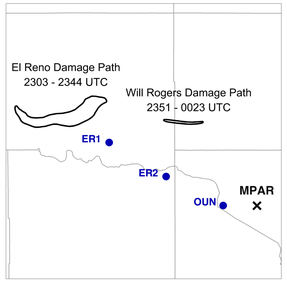

Figure 1. Overview of experiment domain. Damage tracks for the El Reno and Will Rogers tornadoes are plotted in black, with input NME sounding locations indicated by blue circles and the MPAR location marked with "X".

Table 1. Summary of model and data assimilation parameters.

Model	NCOMMAS
Assimilation Technique	LETKF
Ensemble Size	36 Members
Domain	180 x 180 x 20 km, stationary
Δx, Δy	2 km
Vertical Levels, Min Δz	41, 500 m 51, 250 m 61, 125 m
Microphysics	ZVD (Ziegler 1985; Mansell et al. 2010)
Initial Environment	NME 22 UTC Ensemble Mean at (Fig. 1): "ER1" "ER2" "OUN"
Initial Perturbations	u, v – 2.5 m s^{-1} standard deviation
Spread Maintenance	Relax to Prior Perturbation (Zhang et al. 2004) (α = 0.5)
Localization	Gaspari and Cohn (1999)
Observation Error (σ)	Radial Velocity: 2 m s^{-1}, Reflectivity: 5 dBZ
"Cook" Time	20 Min (2200 – 2220 UTC)
Assimilation Window	5 Min, asynchronous

Table 2. Summary of the MPAR dataset used in assimilation.

Quality-Controlled MPAR Data	2221:12 – 2307:32 UTC
Elevation Angles	0.5°, 0.9°, 1.3°, 1.8°, 2.4°, 3.1°, 4.0°, 5.1°, 6.4°, 8.0°
Vertical Cut-off	10 km
Objective Analysis	Cressman, 3(2) km horizontal(vertical) radius of influence
Grid Spacing	6 km
# of 1-Min(5-Min) Volumes Assimilated at: 2240 UTC 2250 UTC 2300 UTC	 18(5) 27(7) 35(9)

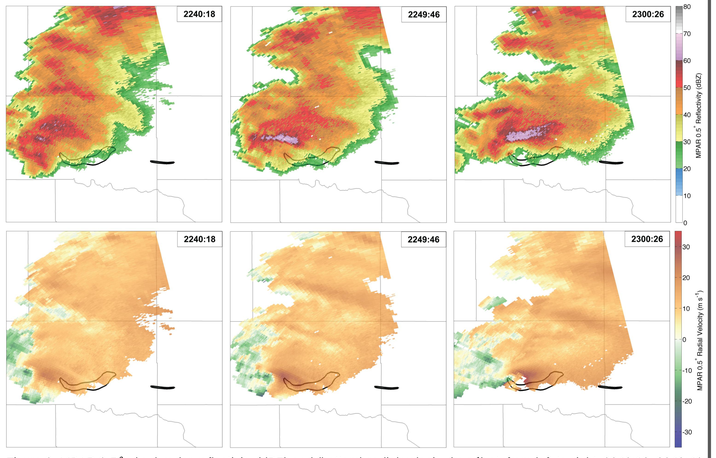

Figure 2. MPAR 0.5° (top) radar reflectivity (dBZ) and (bottom) radial velocity (m s^{-1}) at, from left-to-right, 2240:18, 2249:46, and 2300:26 UTC. El Reno and Will Rogers damage tracks are plotted in black with Oklahoma county borders in gray.

Impact of Vertical Grid Spacing

- Forecasts of the probability of vertical vorticity exceeding a threshold of 0.0125 s^{-1} in the lowest two vertical levels are able to represent the development and initial track of the El Reno tornado ~15 minutes prior to tornadogenesis, but do not predict significant low-level rotation earlier during a period of cell mergers into the forward flank of the El Reno supercell (Figs. 2, 3).
- All forecasts show too rapid movement of the low-level vertical vorticity center and a tendency for cyclic mesocyclogenesis and decay of the El Reno mesocyclone to occur too quickly (Figs. 3, 4).
- Forecasts are found to be sensitive to the number of vertical levels and boundary layer vertical grid spacing in the numerical model (Figs. 3, 4).
- Increasing low-level vertical resolution in the model results in higher probabilities of low-level vertical vorticity and a rightward shift to the probability swath (Figs. 3, 4).
- Increased vertical grid spacing in the boundary layer results in a more accurate representation of the low-level wind field (Fig. 5) and a more favorable wind profile for a strong low-level mesocyclone.

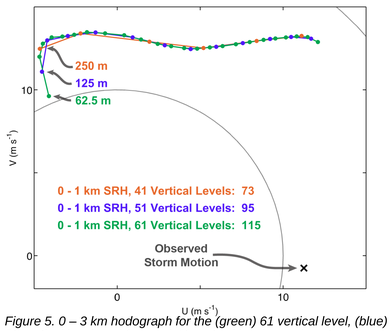

Figure 5. 0 – 3 km hodograph for the (green) 61 vertical level, (blue) 51 vertical level, and (orange) 41 vertical level experiments, respectively. Observed storm motion is denoted by "X".

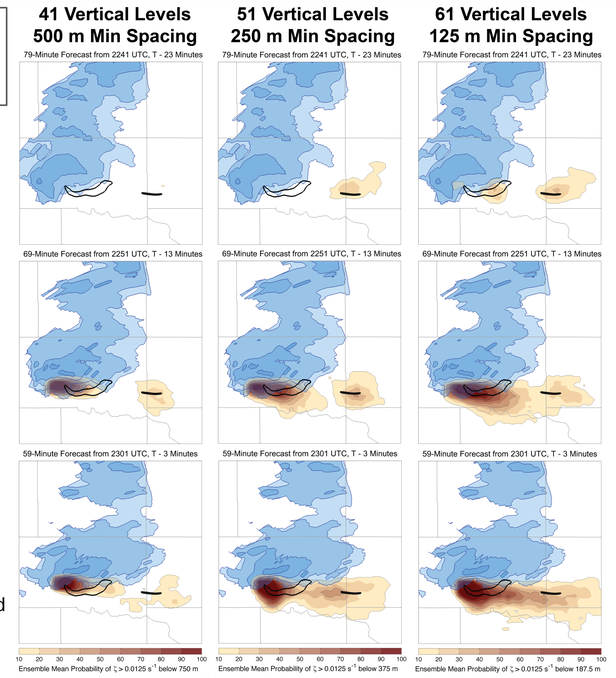

Figure 3. Ensemble mean probabilities of vertical vorticity exceeding 0.0125 s^{-1} in the lowest two model levels for the ER1 input sounding with, from left-to-right, the 41 vertical level, 51 vertical level, and 61 vertical level experiments. Forecasts initialized at 2240, 2250, and 2300 UTC are plotted from top to bottom with contours of 30, 40, 50, and 60 dBZ radar reflectivity from 0.5° MPAR scans at (top) 2240:16, (middle) 2249:46, and (bottom) 2300:26 UTC overlain in blue.

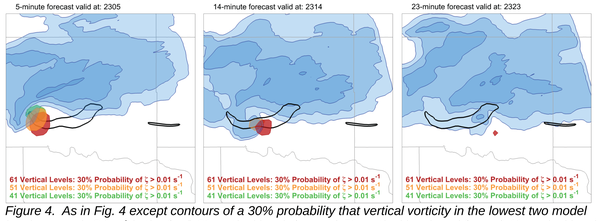

Figure 4. As in Fig. 4 except contours of a 30% probability that vertical vorticity in the lowest two model levels exceeds 0.1 s^{-1} in the (red) 61 vertical level, (orange) 51 vertical level, and (green) 41 vertical level are plotted at (left) 2305, (middle) 2314, and (right) 2323 UTC.

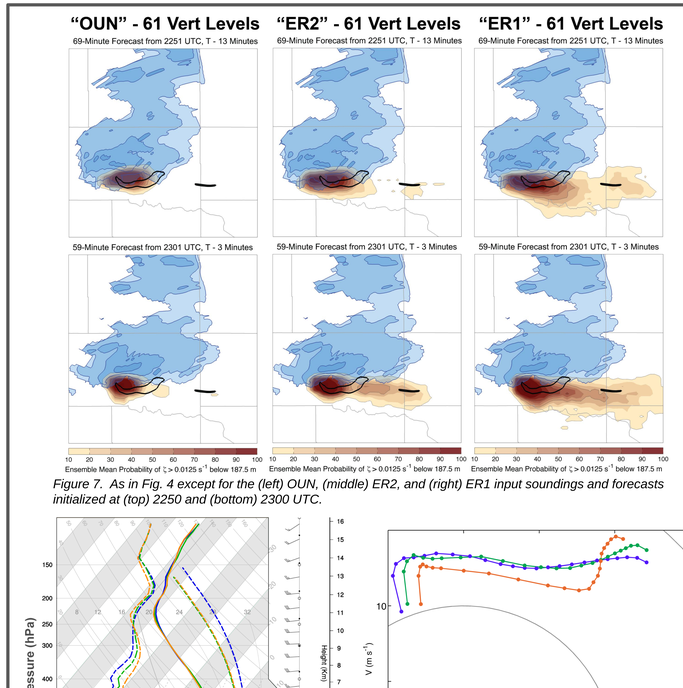

Figure 7. As in Fig. 4 except for the (left) OUN, (middle) ER2, and (right) ER1 input soundings and forecasts initialized at (top) 2250 and (bottom) 2300 UTC.

Figure 8. Skew-T/Log-P diagrams for the (blue) ER1, (green) ER2, and (orange) OUN input soundings.

Figure 9. As in Fig. 3 except for the (blue) ER1, (green) ER2, and (orange) OUN input soundings.

Impact of Initial Environment

- Variation in the location of the input sounding generated by the 22 UTC ensemble mean of the NSSL Mesoscale Ensemble (NME) (Knopfmeier et al. 2014) produce similar variations in the probability of low-level vertical vorticity as changes in the vertical grid spacing (Figs. 1, 3, 7).
- Increasing input sounding distance from the El Reno supercell results in reduced environmental CAPE (Fig. 8) and 0-1 km storm-relative helicity (Fig. 9), and subsequently, lower probabilities of low-level vertical vorticity (Fig. 7).
- The small area of enhanced probabilities of low-level vertical vorticity for the OUN input sounding (Fig. 7) is likely attributable to larger environmental CIN.

← Figure 6. As in Fig. 4 except for 61 vertical level experiments assimilating (left) 5-minute volumes of MPAR data and (right) 1-minute volumes. Forecasts initialized at (top) 2250 and (bottom) 2300 UTC.

Impact of Rapid-Scan PAR Data

- The rapid-scan capabilities of the MPAR allow a more accurate analysis of the El Reno supercell to be produced more quickly (Yussouf and Stensrud 2010; Wicker et al. 2014) and produce higher, more representative probabilities of low-level vertical vorticity than experiments where MPAR data are thinned to one volume per assimilation cycle (Fig. 6).
- Probabilities of vertical vorticity produced by assimilating 1-minute volumes of MPAR data are higher than those produced by 5-minute volumes regardless of the vertical grid spacing employed (not shown).

Summary and Future Work

- Assimilation of rapid-scan MPAR data produces more representative forecasts of low-level vertical vorticity.
- Forecasts of low-level vertical vorticity are sensitive to changes in the initial environment, which can be induced by either model setup (vertical grid spacing) or changes to the input sounding.
- Future work involves further testing the sensitivity of forecasts of the El Reno supercell to initial conditions, transfer of results to a full-physics model in a heterogeneous horizontal environment, and consideration of additional hazards, such as flash flooding, produced by the El Reno supercell.

Acknowledgements

We thank Charles Kuster for his assistance with quality control of MPAR data and Kent Knopfmeier for providing the NME input soundings. The first author was primarily supported by a National Research Council Associateship award at the NOAA/National Severe Storms Laboratory. Additional funding was provided by the NOAA Warn-on-Forecast project.

***Corresponding Author Address: Patrick Skinner, NOAA/NSSL**
120 David L. Boren Blvd., Suite 3333 Norman, OK 72072
patrick.skinner@noaa.gov